Developing laminar flow in a semiporous two-dimensional channel with nonuniform transpiration

M. M. Sorour, M. A. Hassab and S. Estafanous*

A theoretical study of a hydrodynamically and thermally developing flow between an impermeable and a porous plate is presented. The flowing stream is nonuniformly transpired through the porous plate, which is also subjected to a uniform heat flux. The impermeable wall is subjected to a heat loss coefficient to a constant-temperature atmosphere. The inlet to outlet suction ratio, the wall Reynolds number and the Prandtl number were the main system parameters. These parameters were considered in evaluating the axial velocity and pressure distribution, shear stresses, local wall and fluid temperature, and local Nusselt number which characterizes this flow pattern.

Keywords: *developing flow, laminar flow, semiporous medium, nonuniform transpiration, heat transfer, suction*

Introduction

A channel may be said to be uniformly porous when its two walls are porous and the normal velocity at the wall is constant. On the other hand, nonuniform, semiporous channel flow implies that only one wall is porous and the normal velocity at this wall is not constant. Although there are a large number of publications dealing with various combinations of channel flow in porous ducts with suction or injection[1], flow in a semiporous long rectangular duct with nonuniform suction has not previously been investigated.

The present investigation is devoted to a study of the hydrodynamic and heat transfer characteristics of developing flow in a heated, semiporous, long, rectangular channel. Furthermore, in this basic study the heated wall is the porous one, which simulates transpiration cooling. In general, configurations of flow with suction and injection are being increasingly used in modern technology.

Donoughe[2] followed by Eckert *et al*[3] were the first to investigate the hydrodynamics of a fully developed flow in a semiporous channel with uniform suction. In addition, Horton and Yuan[4] investigated the fluid flow in the inlet region of a porous channel with uniform injection.

Carter and Gill[5] investigated the effect of suction and injection on combined free and forced convection in vertical and horizontal channels, the flow being hydrodynamically and thermally developed. On the other hand, Terrill[6], Tsou[7] and Pederson and Kinney[8] studied the thermal entrance problem in a porous channel with uniform suction and injection for various thermal boundary conditions. Furthermore, Raithby[9] investigated the development of the temperature field in the region of fully developed velocity for porous rectangular channels for both constant wall temperature and constant heat flux boundary conditions. Sorour and Hassab[10] investigated a similar problem for a semiporous channel. Lastly, Rhee and Edwards[11] analysed a simultaneous thermally and hydrodynamically developing flow in a long, uniform, semiporous duct.

Analysis

Consider laminar, incompressible fluid flowing axially in a semiporous, long, rectangular close-ended duct as shown in Fig 1. The flow is subjected to nonuniform suction from the porous wall side, such that the flow is completely withdrawn within the length of the duct. The porous wall is subjected to uniform heat flux while the impermeable wall is convective to a constant-temperature wall. In addition, the fluid is assumed to have properties which are independent of the temperature.

An overall mass balance through the duct reveals

$$u_i B = v_{wa} L \tag{1}$$

The dimensionless governing equations of continuity, momentum and energy can be deduced using the dimensionless quantities and Eq (1) to give

$$\frac{\partial U}{\partial X}+\frac{\partial V}{\partial Y}=0 \tag{2}$$

$$U\frac{\partial U}{\partial X}+V\frac{\partial U}{\partial Y}=-\frac{\partial P}{\partial X}+\frac{1}{Re_{wa}}\frac{\partial^2 U}{\partial Y^2} \tag{3}$$

$$U\frac{\partial \theta}{\partial X}+V\frac{\partial \theta}{\partial Y}=\frac{1}{Re_{wa}Pr}\frac{\partial^2 \theta}{\partial Y^2} \tag{4}$$

in which the momentum equation in the Y-direction is neglected, and the second X-derivatives are also neglected.

The boundary conditions imposed on Eqs (1), (2) and (3) are

$$\begin{aligned} &X=0, \quad Y=Y, \quad U=1, \quad V=0, \quad \theta=0\\ &X=X, \quad Y=0, \quad U=0, \quad V=-V_{wx}, \quad \frac{\partial\theta}{\partial Y}=-1\\ &X=X, \quad Y=1, \quad U=0, \quad V=0, \quad \frac{\partial\theta}{\partial Y}=-H_{ua}(\theta_1-\theta_a)\\ &X=L, \quad Y=Y, \quad U=0, \quad V=0 \end{aligned} \tag{5}$$

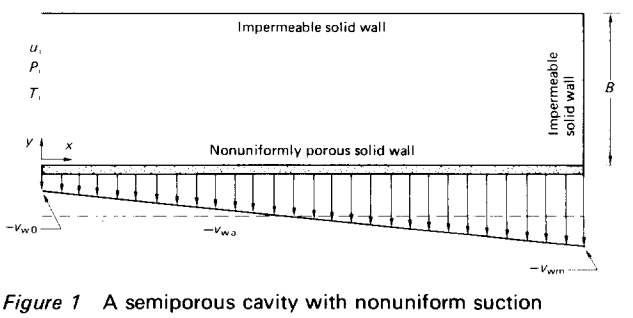

Figure 1 A semiporous cavity with nonuniform suction

* Mechanical Engineering Department, Faculty of Engineering, Alexandria University, Egypt

Received 20 August 1985 and accepted for publication in final form on 14 July 1986

0142-727X/87/010044-11$3.00

At any section X, the term $\partial P/\partial X$ can be considered a function of this distance only. Thus this quantity can be eliminated by differentiating Eq (2) partially with respect to Y. In addition, using Eq (2) we obtain

$$U\frac{\partial^2 U}{\partial X\,\partial Y}+V\frac{\partial^2 U}{\partial Y^2}=\frac{1}{Re_{wa}}\frac{\partial^3 U}{\partial Y^3} \tag{6}$$

Introducing a stream function ψ such that

$$U=\frac{\partial\psi}{\partial Y}$$

$$V=-\frac{\partial\psi}{\partial X} \tag{7}$$

into Eq (6), the resultant equation is

$$\frac{\partial^4\psi}{\partial Y^4}-Re_{wa}\left(\frac{\partial^3\psi}{\partial X\,\partial Y^2}\frac{\partial\psi}{\partial Y}-\frac{\partial^3\psi}{\partial Y^3}\frac{\partial\psi}{\partial X}\right)=0 \tag{8}$$

and, correspondingly, the boundary conditions transform to

$$X=0,\quad Y=Y,\quad \frac{\partial\psi}{\partial Y}=1,\quad \frac{\partial\psi}{\partial X}=0,\quad \psi=-1+Y,\quad \theta=0$$

$$X=X,\quad Y=0,\quad \frac{\partial\psi}{\partial Y}=0,\quad \frac{\partial\psi}{\partial X}=V_{MX},\quad \psi=\psi_X,\quad \frac{\partial\theta}{\partial Y}=-1 \tag{9}$$

$$X=X,\quad Y=1,\quad \frac{\partial\psi}{\partial Y}=0,\quad \frac{\partial\psi}{\partial X}=0,\quad \psi=0,\quad \frac{\partial\theta}{\partial Y}=-H_{ua}(\theta_1-\theta_a)$$

$$V_{wa}=\tfrac{1}{2}(V_{wo}+V_{wm}) \tag{10}$$

$$V_{wx}=V_{wa}+2(1-a)X \tag{11}$$

where a is the inlet suction ratio.

Through using the definitions of the suction Reynolds numbers Re_{wo}, Re_{wm} and Re_{wa}, it follows that

$$Re_{wo}=aRe_{wa} \tag{12a}$$

$$Re_{wm}=(2-a)Re_{wa} \tag{12b}$$

$$Re_{wx}=Re_{wo}+(Re_{wm}-Re_{wo})X \tag{12c}$$

Notation

a	Inlet suction ratio v_{wo}/v_{wa}
B	Depth of the duct
b	Width of the cavity
c_p	Specific heat at constant pressure of the working fluid
H	An elemental length in the Y-direction
h_{ua}	A heat loss coefficient
H_{ua}	A dimensionless heat loss coefficient $\equiv\frac{h_{ua}B}{K}$
K	Conductivity of the fluid
L	Total length of the duct
N_{uL}	A local Nusselt number at the porous wall based on the mean temperature of the fluid inside the duct
p, p_i	Pressure, inlet pressure
P, P_i	Dimensionless pressure $\left(\equiv\frac{p-p_i}{\rho u_i^2}\right)$, dimensionless inlet pressure
Pr	Prandtl number of the working fluid
Po	Power required to maintain the flow
Po^*	Dimensionless power defined by $Po/\rho U_i^2 Q_{in}$
Q_{in}	Volumetric flow rate at inlet
Q_x	Volumetric flow rate at any section x
q_w	Input heat flux per unit length of the porous wall
Re	Reynolds number of the inlet stream $\equiv\frac{u_i(2B)}{\nu}$
Re_{wa}	Average wall Reynolds number $\equiv\frac{v_{wa}B}{\nu}$
Re_{wo}	Wall Reynolds number at the inlet section of the duct $\equiv\frac{v_{wo}B}{\nu}$
Re_{wx}	Wall Reynolds number at location x on the porous wall $\equiv\frac{v_{wx}B}{\nu}$
T, T_i	Temperature, inlet temperature
T_1, T_2	Temperature at location x on the porous and impermeable wall, respectively
T_{EM}	Average fluid temperature at $0.98L$ from inlet
u, u_i	Axial velocity, inlet axial velocity
U	Dimensionless axial velocity $\equiv u/u_i$
U_{AVX}	Dimensionless average sectional axial velocity
v, v_{wa}	Suction velocity and average suction velocity
v_{wo}, v_{wx}, v_{wm}	Suction velocity at $x=0$, $x=x$, and $x=L$, respectively
V	Dimensionless suction velocity $\equiv v/v_{wa}$
V_{wo}, V_{wx}, V_{wm}	Dimensionless suction velocity at $x=0$, $x=x$, and $x=L$; $V_{wo}\equiv v_{wo}/v_{wa}$, $V_{wx}\equiv v_{wx}/v_{wa}$, and $V_{wm}\equiv v_{wm}/v_{wa}$
x	Axial coordinate
X	Dimensionless axial coordinate defined by x/L
y	Transverse coordinate
Y	Dimensionless transverse coordinate $\equiv y/B$
η	Axial coordinate on the impermeable wall
θ	A dimensionless temperature $\equiv\frac{T-T_i}{q_wB/K}$
θ_1, θ_2	Local dimensionless temperature of the porous and impermeable wall, respectively
θ_a	A dimensionless ambient temperature
θ_{MX}	Dimensionless average mean temperature of the fluid inside the duct at the section x
θ_{MAV}	Dimensionless overall mean temperature of the total sucked stream
θ_{MAVX}	Dimensionless overall average mean temperature of the fluid leaving the duct between section $x=0$ and $x=x$
θ_{1AV}, θ_{2AV}	Dimensionless average mean temperature of the porous and impermeable wall, respectively
ν	Kinematic viscosity of the fluid
ρ	Density of the fluid
τ	Shear stress
τ^*	Dimensionless shear stress $\equiv\frac{\tau}{\rho U_i^2}=\frac{2}{Re}\frac{\partial U}{\partial Y}$
ψ	A stream function
ψ^o	An iterative value of the stream function
ψ^N	A better approximation to the value of the stream function
ψ^*	The previous step solution of the function

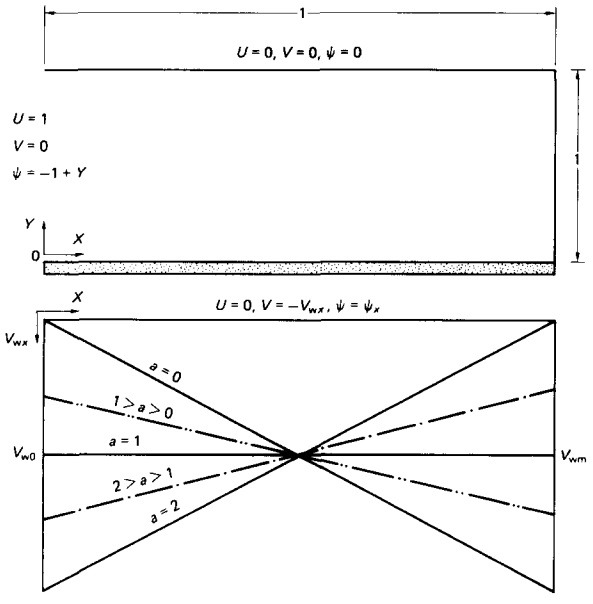

Figure 2 Boundary conditions

$$V_{wx}=-\frac{1}{Re_{wa}}\{Re_{wo}+(Re_{wm}-Re_{wo})X\} \tag{12d}$$

$$\psi_X=-1+\frac{X}{Re_{wa}}\left\{Re_{wo}+\frac{X}{2}(Re_{wm}-Re_{wo})\right\} \tag{12e}$$

$$Re_{wa}=\tfrac{1}{2}(Re_{wo}+Re_{wm}) \tag{12f}$$

Fig 2 shows a schematic diagram of the problem as well as the boundary conditions given by Eq (9). It also illustrates the various linearly varying suction alternatives.

Solution of the momentum equation

The two nonlinear terms of Eq (8) can be quasi-linearized. Let the superscript o denote a previous iteration, and Δ the difference from it, then

$$\frac{\partial\psi}{\partial Y}=\frac{\partial^{\circ}\psi}{\partial Y}+\frac{\partial\Delta\psi}{\partial Y}$$

$$\frac{\partial\psi}{\partial X}=\frac{\partial^{\circ}\psi}{\partial X}+\frac{\partial\Delta\psi}{\partial X}$$

$$\frac{\partial^3\psi}{\partial X\,\partial Y^2}=\frac{\partial^3\psi^{\circ}}{\partial X\,\partial Y^2}+\frac{\partial^3\Delta\psi}{\partial X\,\partial Y^2} \tag{13}$$

$$\frac{\partial^3\psi}{\partial Y^3}=\frac{\partial^3\psi^{\circ}}{\partial Y^3}+\frac{\partial^3\Delta\psi}{\partial Y^3}$$

Then neglecting second-order terms in Δ quantities gives

$$\frac{\partial\psi}{\partial Y}\frac{\partial^3\psi}{\partial X\,\partial Y^2}=\frac{\partial\psi^{\circ}}{\partial Y}\frac{\partial^3\psi}{\partial X\,\partial Y^2}+\frac{\partial\psi}{\partial Y}\frac{\partial^3\psi^{\circ}}{\partial X\,\partial Y^2}-\frac{\partial\psi^{\circ}}{\partial Y}\frac{\partial^3\psi^{\circ}}{\partial X\,\partial Y^2}$$

and (14)

$$\frac{\partial\psi}{\partial X}\frac{\partial^3\psi}{\partial Y^3}=\frac{\partial\psi^{\circ}}{\partial X}\frac{\partial^3}{\partial Y^3}\psi+\frac{\partial\psi}{\partial X}\frac{\partial^3\psi^{\circ}}{\partial Y^3}-\frac{\partial\psi^{\circ}}{\partial X}\frac{\partial^3\psi^{\circ}}{\partial Y^3}$$

Eq (8) is now linearized, and is ready for solution.

A finite difference technique is used for solving this equation. In this method of solution a backward difference approximation is used for the streamwise X derivatives and a central difference one for the cross-stream Y derivatives. Let a superscript * denote a dependent variable at the previous X-step (ie at X_{i-1}), and let the subscript j denote a value at $Y=Y_j$. Since the superscript o denotes the value at a previous iteration, a double superscript comprising o and * denotes the known solution at the previous X-step, ie $\psi_j^{\circ *}=\psi_j^*$. Thus the finite difference formulae for the terms of Eq (8) are

$$\frac{\partial\psi}{\partial X}=\left(\frac{\psi_i-\psi_i^*}{\Delta X}\right)_j$$

$$\frac{\partial\psi}{\partial Y}=\left(\frac{\psi_{j+1}-\psi_{j-1}}{2H}\right)_i$$

$$\frac{\partial^3\psi}{\partial X\,\partial Y^2}=\left(\frac{\psi_{j+1}-2\psi_j+\psi_{j-1}-\psi_{j+1}^*+2\psi_j^*-\psi_{j-1}^*}{\Delta XH^2}\right)_i \tag{15}$$

$$\frac{\partial^3\psi}{\partial Y^3}=\frac{\psi_{j+1}-2\psi_{j+1}+2\psi_{j-1}-\psi_{j-2}}{2H^3}$$

$$\frac{\partial^4\psi}{\partial Y^4}=\frac{\psi_{j+2}-4\psi_{j+1}+6\psi_j-4\psi_{j-1}+\psi_{j-2}}{H^4}$$

Substitution into Eq (8) gives

$$A(j)\psi(j-1)+B(j)\psi(j-1)+C(j)\psi(j)+D(j)\psi(j+1)+E(j)\psi(j+2)=F(j) \tag{16}$$

The constants $A(i), B(i), \ldots, F(j)$ are given by

$$\begin{aligned}
A(j)&=2r-Re_{wa}\{\psi^{\circ}(j)-\psi^*(j)\}\\
B(j)&=-8r+Re_{wa}\{2\psi^{\circ}(j-1)-\psi^*(j+1)-\psi^*(j-1)\}\\
C(j)&=12r+Re_{wa}\{\psi^{\circ}(j+2)-\psi^{\circ}(j+2)\}\\
D(j)&=-8r-Re_{wa}\{2\psi^{\circ}(j+1)-\psi^*(j+1)-\psi^*(j-1)\}\\
E(j)&=2r+Re_{wa}\{\psi^{\circ}(j)-\psi^*(j)\}\\
F(j)&=Re_{wa}[\psi^{\circ}(j+2)\psi^{\circ}(j)-\{\psi^{\circ}(j+1)\}^2\\
&\quad+\{\psi^{\circ}(j-1)^2-\psi^{\circ}(j)\psi^{\circ}(j-2)\}]
\end{aligned} \tag{17}$$

where $r=\Delta X/H^2$, and ΔX and H are the streamwise and cross-stream finite elements, respectively.

The grid system used for solving the momentum equation is shown in Fig 3. In this figure the duct is divided into N_p sections of incremental length ΔX each, and N_p node points. Furthermore each section is divided into n_Y segments in the cross-stream direction, with N_Y+1 node points. The successive application of Eq (16) at any section i yields a system of N_Y-1 simultaneous linear equations in N_Y+1 unknowns. In addition, through the use of the no slip conditions and the application of the momentum equation at the upper and lower walls, two additional equations are given. The following successive iteration scheme is designed for solving the system of linear equations produced by the successive application of Eq (16) at any section i and, hence, the complete solution at this section.

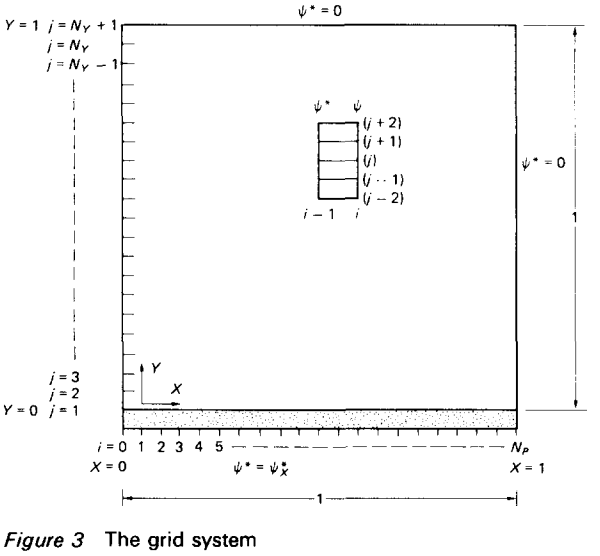

Figure 3 The grid system

(1) Starting with the section $i=1$, at a distance ΔX from the inlet section, the values of ψ^* are already given from the boundary conditions (Eq (9)) for $X=0$.
(2) The values of ψ^o can first be taken equal to the corresponding values of ψ^*.
(3) Having the values of ψ^o and ψ^* the constants given by Eqs (17) can be calculated.
(4) Applying Eq (16) on the node points $j=2, 3, 4, \ldots, N_Y$ of the section under consideration produces a system of N_Y-1 simultaneous linear equations in N_Y-1 unknowns, values of a new variable ψ^N which is a better approximation to the solution than ψ^o.
(5) The system of the simultaneous linear equations produced is then solved simultaneously to yield the values of ψ^N.
(6) The relative differences $1-\psi^o(j)/\psi^N(j)$ are then calculated for all values of $j=2, 3, \ldots, N_Y$.
(7) If any value of the differences calculated in item (6) exceeds the value of a specified accuracy, the values of ψ^o are made equal to the corresponding values of ψ^N, and items (3) through (6) are calculated again.
(8) This procedure continues until the value of any relative difference calculated in item (6) becomes less than the proposed accuracy. At this step the calculated values of ψ^N are considered the required solution, and given the notation ψ^*.
(9) The section under consideration now becomes a known one, and the values of ψ^* obtained in item (8) are then used to obtain the solution of the next section, at a distance ΔX from the former one.
(10) Items (2) through (10) are then iterated until the values of ψ^* are calculated at all sections of the cavity for the given value of Re_{wa} and the inlet suction ratio a.

Now the stream function ψ is determined, the velocity field can be calculated by using Eqs (7) and the suitable approximations given by Eqs (15). Also, any other flow parameter can be determined by the corresponding finite difference approximation. In solving the system of simultaneous linear equations calculated at any section i the method of matrix partitioning was used[11] and r was taken equal to 5 for rapid convergence.

The pressure distribution

An alternative form of the momentum equation is

$$2u\frac{\partial u}{\partial x}+\frac{\partial uv}{\partial y}=-\frac{1}{\rho}\frac{\partial p}{\partial x}+\nu\left(\frac{\partial^2 u}{\partial x^2}+\frac{\partial^2 u}{\partial y^2}\right) \tag{18}$$

Neglecting the second-order x-derivatives and rearranging gives

$$\frac{\partial p}{\partial x}=-\rho\left(2u\frac{\partial u}{\partial x}+\frac{\partial uv}{\partial y}\right)+u\frac{\partial^2 u}{\partial y^2} \tag{19}$$

Since the pressure gradient in the x-direction is a function of the streamwise direction only, the partial derivative can be substituted by the complete derivative. This makes the integration of Eq (19) possible and yields the axial distribution of both the pressure and the pressure gradient.

$$\therefore \frac{dp}{dx}=-\frac{2\rho}{B}\int_0^B u\frac{\partial u}{\partial x}dy+\frac{u}{B}\left(\left.\frac{\partial u}{\partial y}\right|_{y=B}-\left.\frac{\partial u}{\partial y}\right|_{y=0}\right) \tag{20}$$

$$\frac{dP}{dX}=-2\int_0^1 U\frac{\partial U}{\partial X}dY+\frac{1}{Re_{wa}}\left(\left.\frac{\partial U}{\partial Y}\right|_{Y=1}-\left.\frac{\partial U}{\partial Y}\right|_{Y=0}\right) \tag{21}$$

and through introducing the stream function defined by Eqs (8) this transforms to

$$\frac{dP}{dX}=-2\int_0^1 \frac{\partial\psi^*}{\partial Y}\frac{\partial^2\psi^*}{\partial X\,\partial Y}dY+\frac{1}{Re_{wa}}\left(\left.\frac{\partial^2\psi^*}{\partial Y^2}\right|_{Y=1}-\left.\frac{\partial^2\psi^*}{\partial Y^2}\right|_{Y=0}\right) \tag{22}$$

The right hand side of Eq (22) is quite sufficient to determine the values of the pressure gradient $\partial P/\partial X$ at any section X, once the value of ψ^* at this section is known. Simpson's rule is used for calculating the first term on the right hand side of Eq (22), and the following finite difference approximations are used for calculating the second term, which in fact represents the difference in the values of the shear stresses at the upper and lower boundaries respectively.

$$\left.\frac{\partial^2\psi^*}{\partial Y^2}\right|_{Y=1}=\frac{1}{12H^2}\{11\psi^*(N_Y-3)-56\psi^*(N_Y-2)+114\psi^*(N_Y-1)-104\psi^*(N_Y)+35\psi^*(N_Y+1)\} \tag{23}$$

$$\left.\frac{\partial^2\psi^*}{\partial Y^2}\right|_{Y=0}=\frac{1}{12H^2}\{35\psi^*(1)-104\psi^*(2)+114\psi^*(3)-56\psi^*(4)+11\psi^*(5)\} \tag{24}$$

The axial pressure distribution can then be determined by integrating Eq (22), and using the following finite difference approximation:

$$\frac{dP}{dX}=\frac{P|_{X+\Delta X}-P|_X}{\Delta X} \tag{25}$$

from which it follows that

$$P|_{X+\Delta X}=P|_X+\left.\frac{\partial P}{\partial X}\right|_{X+\Delta X}\Delta X \tag{26}$$

Once the pressure at section X, $P|_X$, is known, and the pressure gradient at section $X+\Delta X$, $\partial P/\partial X|_{X+\Delta X}$, is calculated from Eq (22), the pressure at section $X+\Delta X$ can be calculated by using Eq (24). Starting by $P|_X=1$ at the inlet section, the axial pressure distribution can be calculated by the successive substitution of Eq (24), and making use of Eq (20). Furthermore, the shear stress distributions can easily be calculated by using Eqs (21) and (22).

The power required to maintain the motion of the flow can be represented by

$$\Delta Po=-\frac{dp}{dx}Q_x\,dx \tag{27}$$

with

$$Q_x=\bar{u}_x Bb \tag{28}$$

where $\bar{u}_x$ is the average axial velocity at section x.

An overall mass balance to a length x of the channel gives

$$\bar{u}_x=u_i-\frac{1}{B}\int_0^x v_{wx}\,dx \tag{29}$$

$$\therefore Q_x=\left[u_i-\frac{v_{wa}}{B}\left\{ax+(1-a)\frac{x^2}{L}\right\}\right]Bb \tag{30}$$

Combining Eqs (27) and (30) we obtain

$$\Delta Po=-\frac{dp}{dx}\left[u_i-\frac{v_{wa}}{B}\left\{ax+(1-a)\frac{x^2}{L}\right\}\right]Bb\,dx \tag{31}$$

Using the dimensionless parameters and the definition of the stream function we obtain

$$\Delta Po^*=\frac{dP}{dX}\psi_X\,dX \tag{32}$$

$$Po^*=\int_0^1\frac{dP}{dX}\psi_X\,dX \tag{33}$$

Solution of the energy equation

In the solution of the energy equation the method used for approximating the derivatives was similar to the method described for approximating the X and Y derivatives in the momentum equation. The final equation can be written in the following form:

$$B(j)\theta(j-1)+C(j)\theta(j)+D(j)\theta(j+1)=F(j) \tag{34}$$

where the constants $B(j)$, $C(j)$, $D(j)$ and $F(j)$ are

$$B(j)=\frac{-V_j}{2H}-\frac{1}{Re_{wa}PrH^2}$$

$$C(j)=\frac{U_j}{\Delta X}+\frac{2}{Re_{wa}PrH^2}$$

$$D(j)=\frac{V_j}{2H}-\frac{1}{Re_{wa}PrH^2} \qquad (35)$$

$$F(j)=U(j)\frac{\theta_0(j)}{\Delta X}$$

Eq (34) when applied to all the node points $j=1, 2, 3, \ldots, N_Y$ of any section i produces a system of N_Y simultaneous linear equations in N_Y+1 unknown values of the dimensionless temperature θ. Two additional equations can be obtained from the boundary conditions (Eq (9)). This produces a number of equations with an equal number of unknowns. It is to be noted that the method of matrix partitioning is also used for solving the system of simultaneous linear equations.

Heat balance and Nusselt number

At any section x, the bulk mean temperature θ_{MX} is calculated from

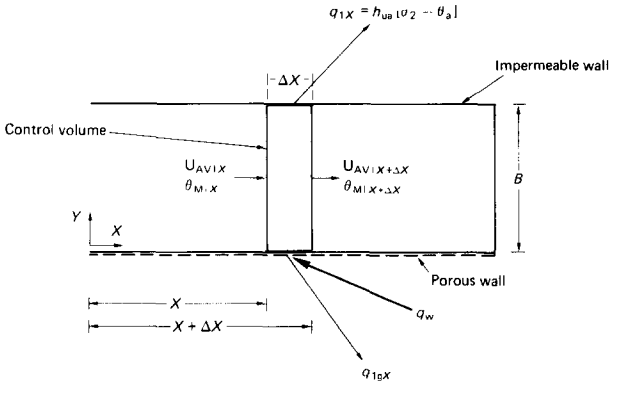

Figure 4 Derivation of the overall bulk mean temperature θ_{MAVX} at section X

$$\theta_{MX}=\frac{1}{U_{AVX}}\int_0^1 U(Y)\theta(Y)\,dY \qquad (36)$$

By using Simpson's rule in the numerical integration of Eq (36) the bulk mean temperature is calculated.

The local heat transfer coefficient is based on the porous wall temperature θ_1 and the bulk mean temperature θ_{MX}, and is defined as

$$N_{uL}=\frac{1}{\theta_1-\theta_{MX}} \qquad (37)$$

For this type of flow, the temperature of the transpired fluid is equal to the temperature of the wall from which transpiration occurs; see the Appendix. However, the overall average mean temperature of the sucked fluid, θ_{MAVX}, can be obtained by the heat balance presented in Fig 4.

$$\frac{q_{Lgx}}{q_w}=1-Re_{wa}Pr\frac{\partial}{\partial X}(U_{AV}\theta_M)_X-H_{ua}(\theta_2-\theta_a)_X \qquad (38)$$

where q_{Lgx}/q_w is the part of heat carried by the transpired fluid per unit length. The total heat energy transported by the sucked fluid, Q_{Lgx} can then be obtained by

$$\frac{Q_{Lgx}}{q_w}=\int_0^x\frac{q_{Lgx}}{q_w}\,dx=Re_{wa}Pr(1-U_{AVX})\theta_{MAVX} \qquad (39)$$

which leads to

$$\theta_{MAVX}=\frac{1}{1-U_{AVX}}\left\{\frac{X}{Re_{wa}Pr}-(V_{AVX}\theta_{MX})-\frac{H_{ua}}{Re_{wa}Pr}\int_0^X(\theta_2-\theta_a)\,dX\right\} \qquad (40)$$

Results and discussion

Hydrodynamic results

The development of the axial velocity profile for different values of inlet suction ratio is presented in Fig 5 for $Re_{wa}=5$ as a representative sample. The effect of suction in decreasing the axial velocity component as well as shifting its peak towards the porous wall with the axial distance is clearly evident, for all values of a. In addition, this trend is more significant for higher Re_{wa}.

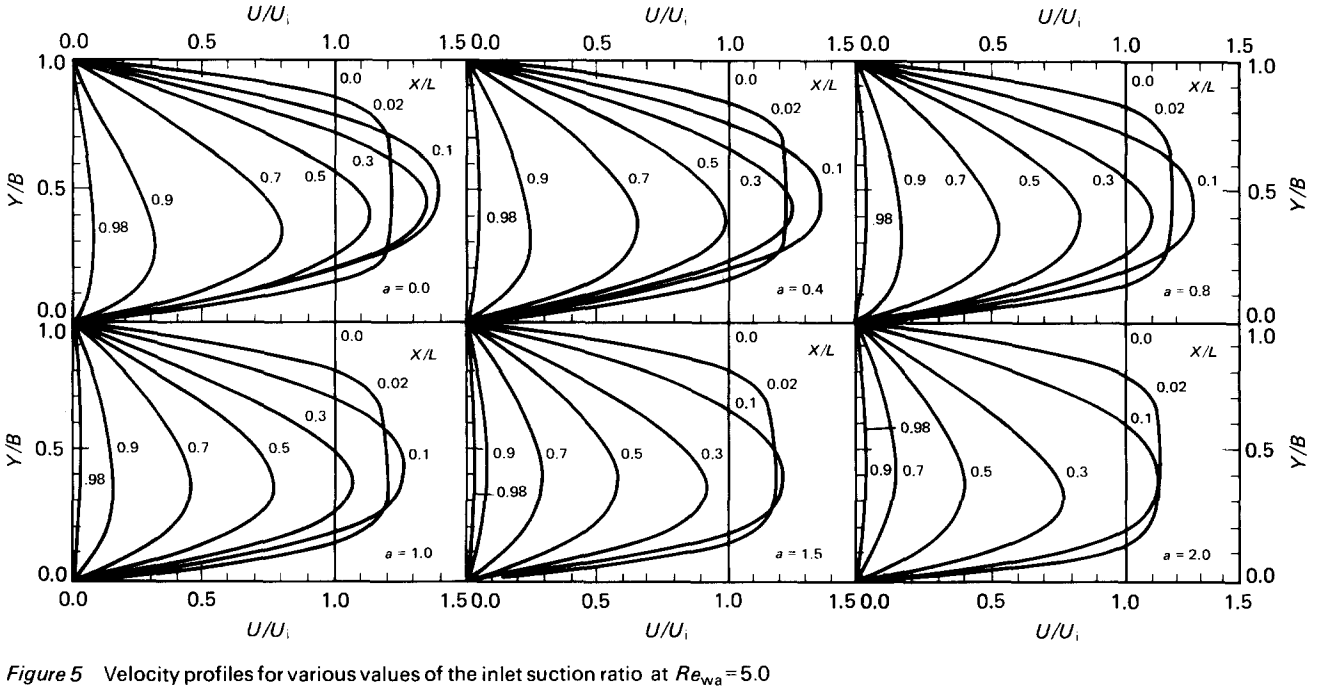

Figure 5 Velocity profiles for various values of the inlet suction ratio at $Re_{wa}=5.0$

Table 1 Maximum values of normalized velocity for $R_{wa}=5$

a	$U/\bar{U}_{max}$	X-location	Y-location
0.0	1.735	0.98	0.26
0.4	1.634	0.98	0.30
0.8	1.567	0.98	0.34
1.0	1.540	0.966	0.38
1.5	1.557	0.350	0.36
2.0	1.599	0.298	0.32

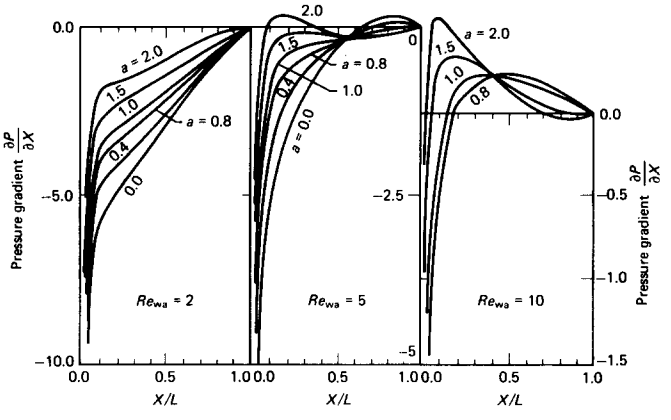

Figure 6 Axial distribution of the pressure gradient for different values of inlet suction ratio a

To determine the characteristics of the flow pattern more closely, a normalized velocity U^* defined by $U^* \equiv U/\bar{U}$ is calculated at different system parameters. These calculations reveal that the flow is semiporous nonuniform flow may be classified into three regions, as follows.

(1) For $0<a<1$, the maximum normalized velocity increases continuously along the x-direction, and reaches its maximum value near the far end of the duct; thus no fully developed velocity profiles are attained.
(2) For $a=1$, the maximum normalized velocity attains a constant value close to the exit section, ie fully developed velocity profiles are attained.
(3) For $1<a<2$, the maximum normalized velocity increases along the x-direction until it reaches a maximum value at some location, but decreases again beyond this location, ie no fully developed velocity profiles are attained.

Table 1 shows the maximum values of the normalized velocity for different values of a and $R_{wa}=5$.

This phenomenon is also illustrated in the axial distribution of the pressure gradient presented in Fig 6. The pressure gradient for various inlet suction ratios and three wall Reynolds numbers reveals that for $a=1$ a linear relationship is established at some downstream axial distance. This is more clearly seen for low values of Re_{wa}, where the linearity is sustained over a greater part of the length of the duct. Conversely, this linearity of the axial pressure gradient is not realized for $a=1$. This supports the conclusion that a fully developed velocity region only eists for uniform suction.

The nonexistence of a fully developed velocity profiles appears more clearly as Re_{wa} increases. In addition, at these higher-values of Re_{wa} pressure recovery prevails, especially for high values of a. Fig 7 presents the pressure distribution for various system parameters, illustrating another feature of this type of flow. This pressure recovery reduces the pumping power required to maintain the flow compared with its equivalent flow between two impermeable walls. Table 2 presents a sample of these results which indicate that the dimensionless pumping power decreases with increase in the inlet suction ratio and also the suction Reynolds number.

The axial distribution of the shear stresses at the porous and impermeable walls for various values of inlet suction ratio and average wall Reynolds number are presented in Fig 8. At the porous wall, suction increases the negative values of shear

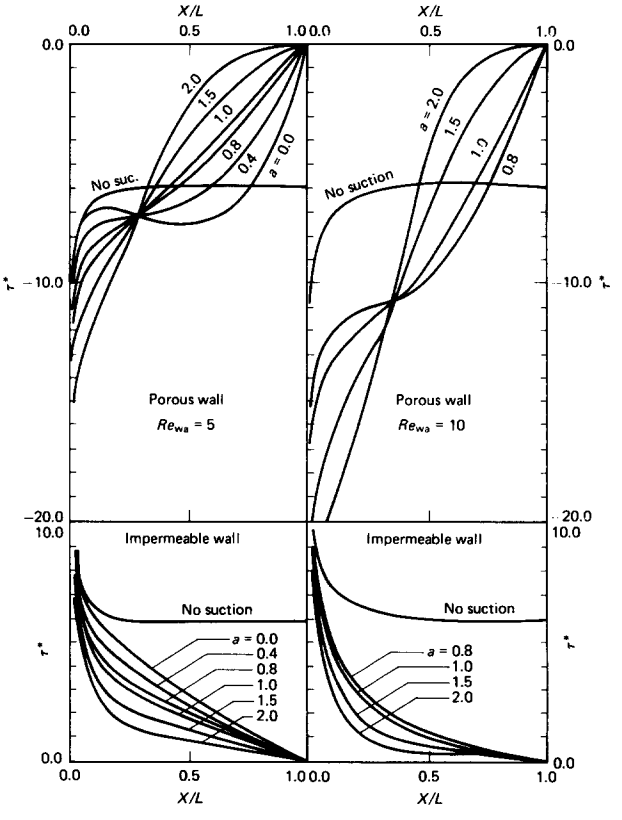

Figure 7 Pressure distribution for different values of inlet suction ratio a

Table 2 Pumping power Po^* for varying Re_{wa} and a

	Po^*	
a	$Re_{wa}=5.0$	$Re_{wa}=10.0$
0.0	0.9715	Separation
1.0	0.47136	0.13283
2.0	0.18959	0.00371
No suction	2.75690	1.55789

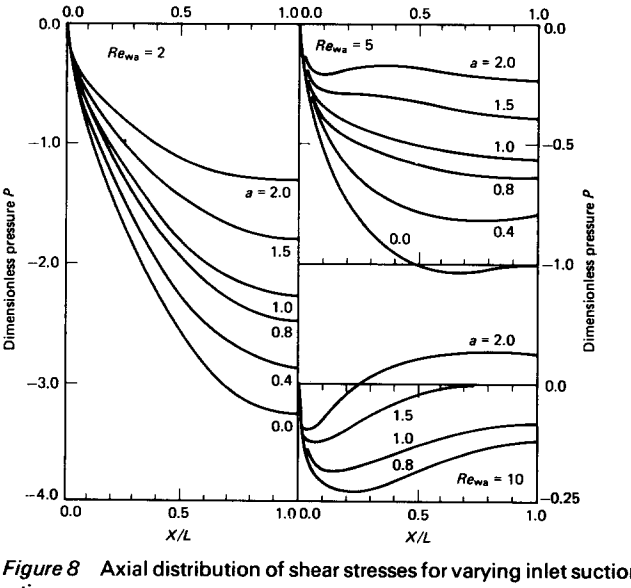

Figure 8 Axial distribution of shear stresses for varying inlet suction ratio a

stresses at the inlet section but decreases them further downstream. On the other hand, suction decreases the shear stresses at the impermeable wall over the whole channel length.

Suction causes a large portion of the flowing mass to flow in a narrow region near the wall from which the fluid is being sucked. Therefore, the velocity gradient in this region increases, and, consequently, so do the shear stresses. However, as the flow proceeds in the axial direction, the mass concentration near this wall, and hence the transverse velocity gradient, diminishes, which explains the reduction in the shear stresses at the porous wall in the far end region of the duct.

The reduction of the shear stresses at the impermeable wall may cause separation when zero values are reached. Therefore, for a given value of the inlet suction ratio, there is a maximum value of the average wall Reynolds number, beyond which separation occurs. Table 3 indicates these maximum permissible values.

Table 3 Maximum values of Re_{wa} without separation at the impermeable wall

a	Re_{wa}
0.0	7.1
0.8	11.5
1.0	13.2
2.0	14.5

The results of separation for uniform suction ($a=1$) inside a semiporous rectangular duct agree with the results of previous investigations[2,8]. However, nonuniform suction increases average permissible Reynolds number when $a>1$.

Thermal results

In this section the effect of suction on the temperature distribution of the porous and impermeable walls, the exit fluid temperature, and the Nusselt numbers at the porous wall are presented for Reynolds numbers $2<Re_{wa}<10$ and for various inlet suction ratios $0<a<2$. The first subsection deals with an adiabatic impermeable wall, while the second deals with a nonadiabatic wall.

Impermeable adiabatic wall

Fig 9 presents the axial temperature distribution of the porous and impermeable walls with various inlet suction ratios and for two representative values of Re_{wa}. For higher inlet suction ratios the cooling effect is highest at the inlet section, and lowest at the exit sections. Generally, transpiration cools these walls

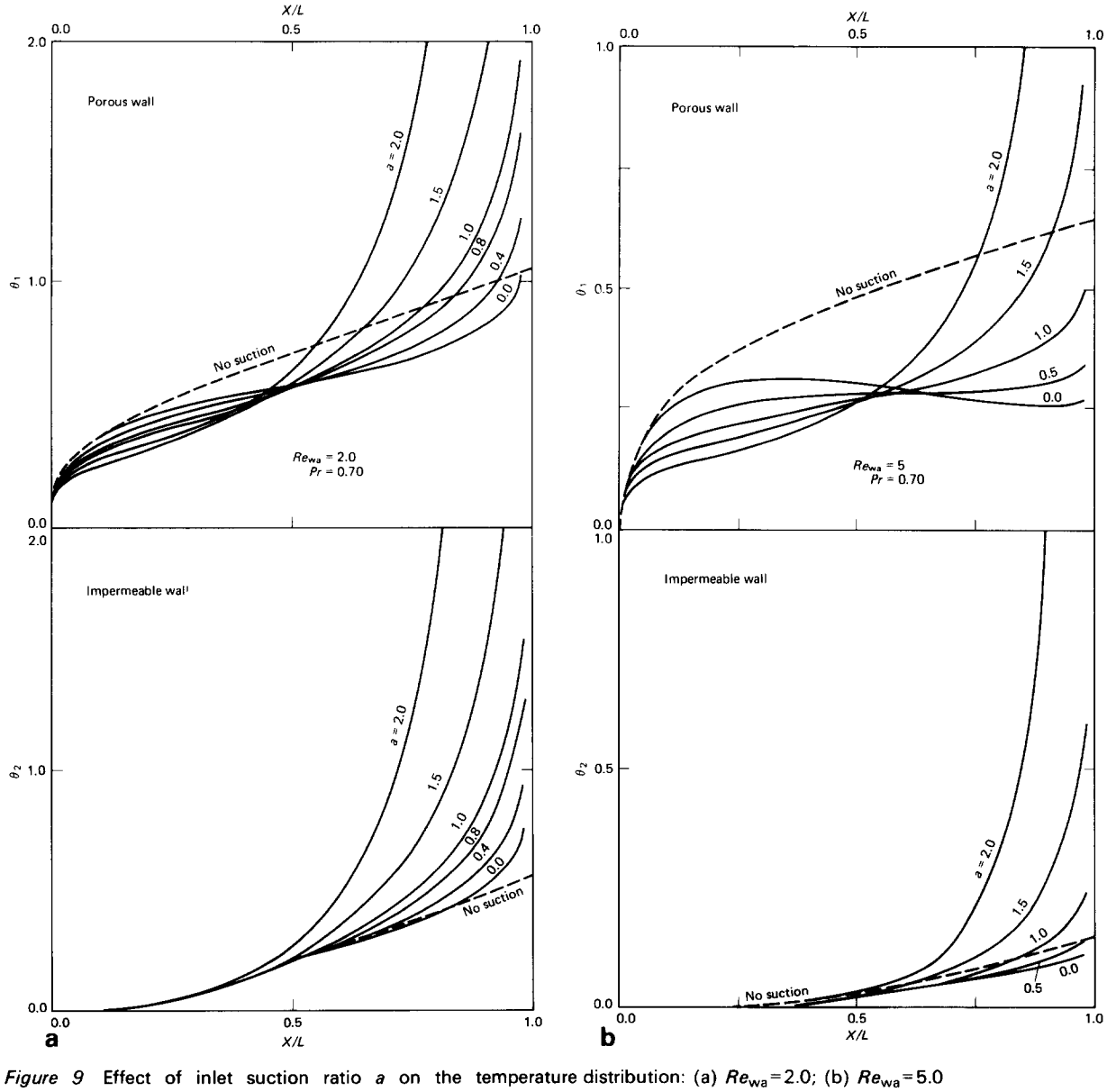

Figure 9 Effect of inlet suction ratio a on the temperature distribution: (a) $Re_{wa}=2.0$; (b) $Re_{wa}=5.0$

Table 4 Values of θ_1, θ_2 and θ_{MAV} for different values of the inlet suction ratio and wall Reynolds number

	$Re_{wa}=2$			$Re_{wa}=5$			$Re_{wa}=10$		
a	θ_{MAV}	θ_{1AV}	θ_{2AV}	θ_{MAV}	θ_{1AV}	θ_{2AV}	θ_{MAV}	θ_{1AV}	θ_{2AV}
0.0	0.68548	0.57369	0.22247	0.27384	0.27328	0.03538	Separation in the velocity field		
0.4	0.68535	0.58819	0.24180	0.27382	0.26295	0.03634	Separation in the velocity field		
0.8	0.68528	0.62058	0.27673	0.27382	0.26267	0.04135	0.13654	0.13530	0.00505
1.0	0.68528	0.64748	0.30392	0.27383	0.26729	0.04638	0.13763	0.13561	0.00606
1.5	0.68546	0.78314	0.43779	0.27399	0.30373	0.07690	0.13637	0.14981	0.01318
2.0	0.68733	1.66288	1.31182	0.27494	0.53998	0.29512	0.13628	0.28072	0.11719
No suction	0.68263	1.63059	0.54582	0.27413	0.45646	0.04940	0.13850	0.19192	0.00488
$1/Re_{wa}Pr$	0.6944			0.2777			0.13888		

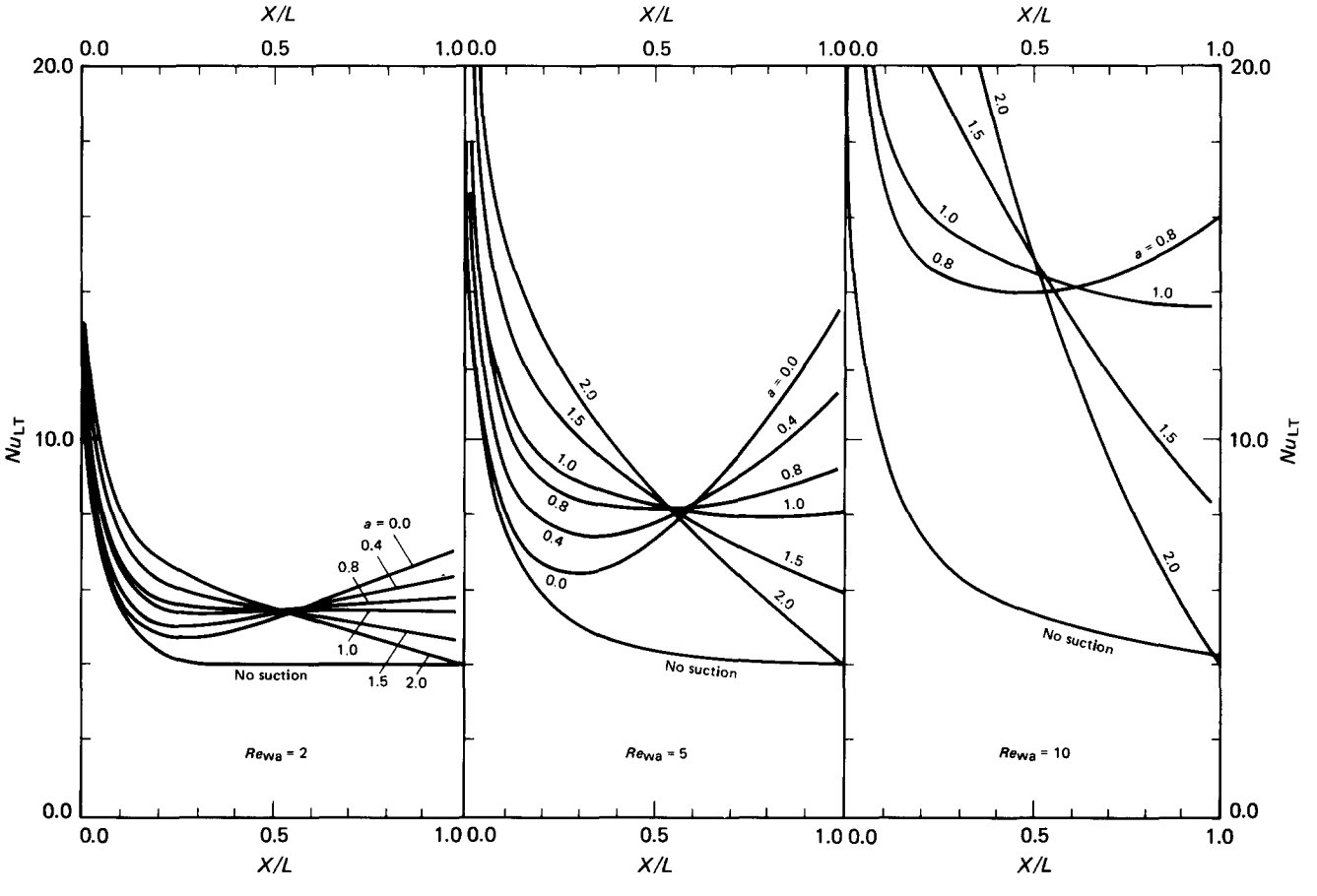

Figure 10 Nusselt numbers for different values of the suction Reynolds number

compared with flow between impermeable walls, except at high suction ratios where higher temperatures are observed at the exit sections of the duct.

The average values of the wall temperature as well as the overall bulk mean temperature of the fluid leaving the cavity are given in Table 4. Increasing the inlet suction ratio from $a=0$ has no immediate effect on the temperature of the two walls, up to a certain value of a, which is dependent on Re_{wa}, where a substantial increase is observed. Conversely, increasing Re_{wa} decreases the mean temperatures of the two walls and the exit fluid temperature.

Fig 10 presents the effect of nonuniform suction on the local Nusselt numbers at the hot porous wall for various wall Reynolds numbers. It can be seen that for uniform suction, ie $a=1$, an asymptotic constant value of Nusselt number characterizes the thermally stabilized section. In addition, the length of this section decreases as Re_{wa} increases. Conversely for nonuniform suction, $a-1$, thermal stabilization is not attained.

Comparing these results with the corresponding ones for heat transfer between impermeable walls, it can be seen that all combinations of nonuniform and uniform suction produce higher heat transfer rates. However, there is an advantageous feature for nonuniform suction, especially for $a<1$. In this case the known decreasing trend of the local Nusselt number with the axial distance is superimposed on a linearly increasing function due to the suction rate. Consequently, the resultant characteristic curve attains a minimum value at some axial distance within the duct, but at the exit section very high heat transfer rates are established.

Nonuniform suction changes the flow rate with the axial distance, which has a hydrodynamic effect on the convective heat transfer. However, the thermal effect of the lateral convective heat transfer coefficient is much more dominant. This is the reason why the increase in wall Reynolds number is characterized by an equivalent increase in the Nusselt number, and why with suction rate increasing with the axial distance the Nusselt number at the exit section is very high.

Comparison of the present results with those previously published is only possible at uniform suction[11]. However, since Rhee *et al*[11] did not present the mean fluid temperature which

could indicate the accuracy of the results when compared with its expected value of $1/Re_{wa}Pr$, it is difficult to explain the small difference between these results. On the other hand, referring to Table 3 it can be seen that the present results are fairly accurate and that the accuracy increases with the suction Reynolds number.

For completeness, it is interesting to note that the fully developed Nusselt number for semiporous uniform suction flow is lower than its equivalent in porous uniform suction flow. For $Re_{wa}=5$, $Pr=0.72$ the fully developed Nusselt number in the present investigation is equal to 8.2 compared with 16.51 in Ref 7.

Table 5 Comparison between investigations

	$Re_{wa}=2$		$Re_{wa}=10$	
Investigation	θ_{1AV}	θ_{2AV}	θ_{1AV}	θ_{2AV}
Rhee *et al*[11]	0.7153	0.3646	0.1427	0.0085
Present	0.6474	0.3039	0.1356	0.0067

Table 6 Average heat losses from the impermeable wall for different values of dimensionless heat loss coefficient at $Re_{wa}=5$

	Average heat losses q_{LAV}/q_w		
a	$H_{ua}=1.0$	$H_{ua}=10$	$H_{ua}=50$
0.0	0.022985	0.052543	0.059354
0.5	0.023839	0.052839	0.059120
1.0	0.029102	0.061608	0.068269
1.5	0.045613	0.088316	0.096234
2.0	0.117914	0.170974	0.179242
No suction	0.037949	0.113162	0.137217

Impermeable convective wall

In this subsection we describe the thermal characteristics of this flow when the upper impermeable wall loses heat to a constant-temperature atmosphere, which is more realistic in terms of engineering applications. For that purpose the Biot number, ie the dimensionless heat loss coefficient, varied from 1 to 50, which covers a large range of boundary conditions and approaches the extreme case of a fixed-temperature wall.

Fig 11 presents the ratio of heat losses to the heat input on the porous wall versus the axial distance for three inlet suction ratios and various heat loss coefficients. At the entrance the heat loss is independent of suction ratios. Conversely, at the exit, high suction ratios give rise to much higher heat losses that the corresponding small suction ratios and, indeed, the no-suction case. In fact, if the average heat losses from the impermeable wall shown in Table 6 are considered, it can be seen that minimal heat loss is attained at zero suction ratio.

Table 7 shows the effect of wall Reynolds number on the heat losses from the impermeable wall. For the results shown in this table, heat input to the duct was constant and heat flux varied since different channel lengths were chosen to satisfy the condition of a closed-ended duct with different suction Reynolds numbers. It can be seen that for $a<1$, increasing Re_{wa} reduces considerably the average heat losses from the cavity and hence improves the thermal performance of the flow. However this is not true for $a>1$.

The effect of fluid properties was investigated by studying the influence of changing the Prandtl number on the thermal characteristics. Table 8 presents the average wall temperature and exit fluid temperature at various Prandtl numbers for a sample of the results at two extreme conditions of adiabatic impermeable wall and maximum heat loss condition respectively. It can be seen that increasing the Prandtl number cools the porous and the impermeable walls and reduces the exit fluid temperature. This cooling effect is reflected in a reduction of the heat losses from the impermeable wall. At $Pr=10$ there is

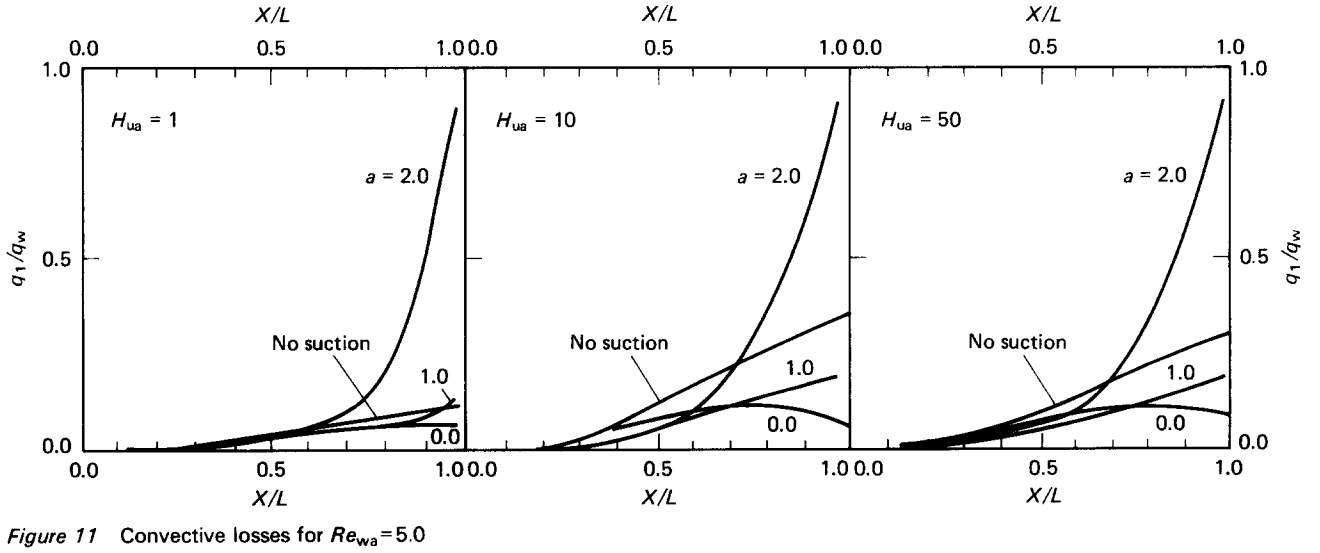

Figure 11 Convective losses for $Re_{wa}=5.0$

Table 7 Average heat losses from the upper wall for different values of Re_{wa} and a ($Re=2000$, $Pr=0.72$, $H_{ua}=50$)

	$Re_{wa}=2$		$Re_{wa}=5$		$Re_{wa}=10$	
a	q_{LAV}	θ_{MAV}	q_{LAV}	θ_{MAV}	q_{LAV}	θ_{MAV}
0.0	0.264281	0.503971	0.148385	0.6448	Separation in the velocity field	
1.0	0.286621	0.488329	0.170673	0.63738	0.054045	0.674672
2.0	0.383744	0.421331	0.448105	0.55995	0.43215	0.619165

Table 8 Effect of the Prandtl number on the average fluid and wall temperatures ($Re_{wa}=5$, $a=1$, $H_{ua}=50$)

Pr	q_{LAV}	θ_{MAV}	θ_{1AV}	θ_{2AV}
0.1	0.949417	0.976869	0.974777	0.018794
0.10	0.620450	0.745532	0.742190	0.012246
0.72	0.068269	0.254948	0.253732	0.001327
1.00	0.029658	0.191201	0.190871	0.000574
2.00	0.00196	0.098034	0.098568	0.000037
10.00	0.000000	0.015234	0.015365	0.000000

($Re_{wa}=5$, $a=1$, $H_{ua}=0.0$)

Pr	θ_{MAV}	θ_{1AV}	θ_{2AV}
0.01	19.691716	17.78520	17.34100
0.1	1.970325	1.807990	1.406690
0.72	0.272493	0.267290	0.046380
5.0	0.037617	0.037935	0.0000
10.0	0.015239	0.01537	0.0000

no difference between the temperatures of the walls and the fluid for the insulated wall case and those for the convective one.

Therefore, transpiring high Prandtl number fluids is thermally attractive. In addition, using small inlet suction ratios will allow the transpiration of more viscous fluids since the suction velocity increases as the viscosity decreases with heating downstream in the duct.

Conclusions

A finite difference analysis of the forced convective flow between a nonporous and a porous parallel plate with nonuniform suction is described. The impermeable plate convects heat to a constant-temperature atmosphere and the porous plate was subjected to constant heat flux.

Nonuniform suction produces a continuously developing flow in the whole length of the duct. Large inlet suction ratio is recommended for hydrodynamic applications. The pressure recovery encountered under these flow conditions reduces the pumping power. In addition, higher permissible wall suction Reynolds numbers can be obtained. On the other hand, for heating applications, small inlet suction ratio is recommended. Higher heat transfer rates to the working fluid, and lower heat losses to the environment, are encountered in this condition for the same heat input, wall Reynolds number and heat loss coefficient.

References

1 Yeroshenko, V. M., Zaichik, L. I. and Bakhvalov, B. Yu. Heat transfer in laminar plane channel flow with uniform suction or injection. *Int. J. Heat Mass Transfer* 1981, **24**(10), 1649

2 Donoughe, P. L. Analysis of Laminar Incompressible Flow in Semiporous Channels. NACA Tech Note 3795, 1956

3 Eckert, E. R. G., Donoughe, P. L. and Moore, B. J. Velocity and Friction Characteristics of Laminar Viscous Boundary-layer and Channel Flow over Surfaces with Injection or Suction. NCA Tech Note 41-2, 1957

4 Horton, T. E. and Yuan, S. W. Laminar flow in the entrance region of a porous-wall channel. *Appl. Sci. Res. Sec A*, 1965, **14**(4), 233–249

5 Carter, L. F. and Gill, W. N. Asymptotic solution for combined free and forced convection in vertical and horizontal conduits with uniform suction and blowing. *A.I. Ch. E.J.* 1964, **10**(3), 330–339

6 Terrill, R. M. Heat transfer in laminar flow between parallel porous plates. *Int. J. Heat Mass Transfer* 1965, **8**, 1491–1497

7 Tsou, R. C. H. On the linearized analysis of entrance flow in heated, porous conduits. *Int. J. Heat Mass Transfer* 1976, **19**, 445–448

8 Pederson, R. J. and Kinney, R. B. Entrance-region heat transfer for laminar flow in porous tubes. *Int. J. Heat Mass Transfer* 1971, **14**, 159–161

9 Raithby, G. Laminar heat transfer in the thermal entrance region of circular tubes and two dimensional rectangular ducts with wall suction and injection. *Int. J. Heat Mass Transfer* 1971, **14**(2), 223–243

10 Sorour, M. M. and Hassab, M. A. Effect of sucking the hot fluid film on the performance of flat plate collector. *Appl. Energy* 1983, **14**, 161–173

11 Rhee, S. J. and Edwards, D. K. Laminar entrance flow in a flat plate duct with asymmetric suction and heating. *Numerical Heat Transfer*, 1981, **4**, 85–100

Appendix: Demonstration that the temperature of the transpired fluid is equal to the wall temperature from which transpiration occurs

An alternative form of the energy equation (Eq (4)) is given by

$$\frac{\partial(U\theta)}{\partial X}+\frac{\partial(V\theta)}{\partial Y}=\frac{1}{Re_{wa}Pr}\frac{\partial^2\theta}{\partial Y^2} \tag{A1}$$

Integrating Eq (A1) along one section X, from $Y=0$ to $Y=1$, it follows that

$$\int_0^1\frac{\partial(U\theta)}{\partial X}\,dY+\int_0^1\frac{\partial V\theta}{\partial Y}dY=\frac{1}{Re_{wa}Pr}\int_0^1\frac{\partial^2\theta}{\partial Y^2}\,dY \tag{A2}$$

Carrying out the integration, and using the identity

$$\int_0^1 U\theta\,dY=U_{AVX}\theta_{MX} \tag{A3}$$

Eq (A2) gives

$$\frac{d}{dX}(U_{AVX}\theta_{MX})+(V\theta)\Big|_{Y=0}^{Y=1}=\frac{1}{Re_{wa}Pr}\left(\frac{\partial\theta}{\partial Y}\right)\Big|_{Y=0}^{Y=1}$$

or

$$\frac{d}{dX}(U_{AVX}\theta_{MX})+V_{WX}\theta_1=\frac{1}{Re_{wa}Pr}\left(\frac{\partial\theta}{\partial Y}\Big|_{Y=1}-\frac{\partial\theta}{\partial Y}\Big|_{Y=0}\right)$$

$$\theta_1=\frac{1}{V_{WX}}\left\{\frac{1}{Re_{wa}Pr}\left(\frac{\partial\theta}{\partial Y}\Big|_{Y=1}-\frac{\partial\theta}{\partial Y}\Big|_{Y=0}\right)-\frac{d}{dX}(U_{AVX}\theta_{MX})\right\} \tag{A4}$$

Now, assuming the temperature of the sucked fluid at location X on the porous wall is θ_{gx}, then a heat balance made on the control volume shown in Fig A1 gives

$$-K\frac{\partial T}{\partial y}\Big|_{y=0}\Delta X+\rho cpBu_{AV}|_X T_M|_x$$

$$=\rho cpBu_{AV}|_x T_M|_x+\rho cpB\frac{\partial}{\partial X}(u_{AV}|_x T_M|_x)\Delta X$$

$$-K\frac{\partial T}{\partial y}\Big|_{y=B}\Delta X+\rho cpv_{wx}\Delta X(T_{gx}-T_i)$$

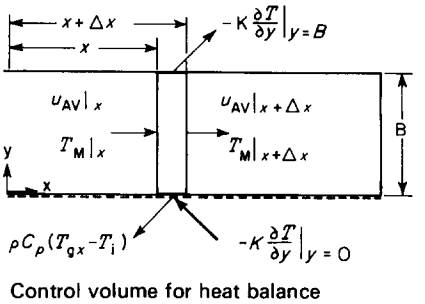

Figure A1 Control volume for heat balance

Rearranging, we have

$$-K\left.\frac{\partial T}{\partial y}\right|_{y=0}=\rho cpB\frac{\partial}{\partial x}(u_{AV}|_x\theta_M|_x)-K\left.\frac{\partial T}{\partial y}\right|_{y=B}+\rho cpv_{wx}(T_{gx}-T_i) \quad (A5)$$

Introducing the dimensionless parameters gives

$$\rho cpV_{WX}V_{WA}\frac{q_wB}{K}\theta_{gX}=-\rho cpB\frac{1}{L}\frac{\partial}{\partial x}\left(U_iU_{AVX}\frac{q_wB}{K}\theta_{MX}\right)-\frac{K}{B}\frac{q_wB}{K}\left.\frac{\partial\theta}{\partial Y}\right|_{Y=0}+\frac{K}{B}\frac{q_wB}{K}\left.\frac{\partial\theta}{\partial Y}\right|_{Y=1}$$

Rearranging gives

$$\rho cpV_{WA}V_{WX}\theta_{gX}=\frac{K}{B}\left(\left.\frac{\partial\theta}{\partial Y}\right|_{Y=1}-\left.\frac{\partial\theta}{\partial Y}\right|_{Y=0}\right)-\frac{\rho cpBU_i}{L}\frac{\partial}{\partial X}(U_{AV}\theta_M)_X$$

or

$$V_{WX}\theta_{gX}=\frac{K}{\rho cpBV_{WA}}\left(\left.\frac{\partial\theta}{\partial Y}\right|_{Y=1}-\left.\frac{\partial\theta}{\partial Y}\right|_{Y=0}\right)-\frac{BU_i}{LV_{WA}}\frac{\partial}{\partial X}(U_{AV}\theta_M)_X$$

$$=\frac{1}{Re_{wa}Pr}\left(\left.\frac{\partial\theta}{\partial Y}\right|_{Y=1}-\left.\frac{\partial\theta}{\partial Y}\right|_{Y=0}\right)-\frac{\partial}{\partial X}(U_{AV}\theta_M)_X$$

from which,

$$\theta_{gX}=\frac{1}{V_{WX}}\left\{\frac{1}{Re_{wa}Pr}\left(\left.\frac{\partial\theta}{\partial Y}\right|_{Y=1}-\left.\frac{\partial\theta}{\partial Y}\right|_{Y=0}\right)-\frac{\partial}{\partial X}(U_{AV}\theta_M)_X\right\} \quad (A6)$$

Comparing Eqs (A4) and (A6) shows that

$$\theta_{gX}=\theta_i$$

ie, the temperature of the sucked fluid is equal to the temperature of the wall from which suction occurs; this is true at any location X on the transpirating wall.

Book review

HEAT TRANSFER 1986 — Proceedings of the Eighth International Heat Transfer Conference

Eds C. L. Tien, V. P. Carey and J. K. Ferrell in cooperation with the members of the International Scientific Committee and the US Scientific Committee

These proceedings include two plenary papers (one on the history of early conferences and the other on appreciation of the work of D. G. Fahrenheit), 28 keynote papers by various authorities on selected topics, 450 contributed papers, an author index, a subject index and a common nomenclature, comprising six volumes and 3193 pages.

Heat transfer is a sufficiently active field to support several prestigious journals and annual conferences. Hence, these Proceedings of the 8th International Conference are representative of current work rather than a compilation of work over the four years since the last conference. Even so, the quantity, international scope and general high quality of the contents makes access to these six volumes sine qua non to everyone working in the field of heat transfer.

The editors, conference committees and the publisher are to be commended for carrying out the process of review, selection, and publication over a very short span of time, thereby making the contents quite timely. The restriction of the contributed papers to six pages appears to have resulted in progress reports and/or in the omission of essential information in only a few instances. The preparation of the printed version on mats by the authors resulted in more typographical and other errors than an edited journal set in type. Also, a variation from paper to paper in type face, contrast and readability is quite evident. Fortunately, almost all of the pages fall within the range of decipherability.

The authorship of the keynote papers assures their authenticity. As such, they are invaluable as reviews or reports on the state of the art. The only disappointment is not to fine one in your subject of interest.

The contributed papers encompass a wider range of quality, perhaps as a consequence of a variability in the standards imposed by the several independent national committees. One might expect to gain some insight into the new directions of technology by surveying these papers, but such trends are not evident to this reviewer. Indeed, one might infer that the art and science of heat transfer are undergoing only a very gradual transition. This may imply a period of consolidation in which well-established methods of analysis such as machine computation, and modern techniques of measurement such as laser-Doppler anemometry are being widely applied to transform heat transfer from a semi-quantitative field, as reflected by log–log plots of widely scattered data, to a profession with a pervasive theoretical and a sound experimental basis.

A detailed analysis of content and trends is hardly feasible here, but several selective observations are offered as follows. Some techniques from other fields are being adapted for improved measurement. Research on heating and cooling is obviously in at least temporary eclipse. Research is apparently interfacial effects, boiling in flow and two-phase convection. Nuclear and augmented heat transfer remain popular topics but the number of papers on electronic, biological and medical aspects of heat transfer is conspicuously and surprisingly small.

One subtle aspect of the contents is the internationality of these volumes. One might classify national contributions by their typographical quality but not by their scientific content. This group of papers is strong evidence that in heat transfer the ideal of 'one world' is now closely approximated.

The lingering impression of these volumes, on this reviewer, is the magnitude and quality of the work. Anyone who has a broad interest in heat transfer will be almost overwhelmed by the essential task of assimilating this new material.

The price of the complete set, while not necessarily excessive, is a strong incentive to attend the Ninth Conference and thereby obtain the proceedings as part of the registration fee.

Stuart W. Churchill
Carl V. S. Patterson Professor of Chemical Engineering,
The University of Pennsylvania,
Philadelphia, PA, USA

Published price $585.00 by Hemisphere Publishing Corporation, Berkeley Building, 19 W 44th Street, New York, NY 10036, USA.